Guidelines for Hemispherical Feature Inspection Using Coordinate Measuring Machines

Boonchai Techaroongruengkij[1] and Chakguy Prakasvudhisarn*[2]
[1]School of Manufacturing Systems and Mechanical Engineering, Sirindhorn International Institute of Technology, Thammasat University, Pathum Thani, 12121, Thailand
[2]School of Technology, Shinawatra University, Shinawatra Tower III, 15th floor, 1010 Viphavadi Rangsit Rd., Chatuchak, Bangkok, 10900, Thailand,
Email: chakguy@shinawatra.ac.th

Abstract

To increase efficiency and effectiveness of form inspection using probe-type coordinate measuring machines (CMMs) on hemispherical feature, a data collection problem consisting of sample sizes, sample point locations, and sampling sequences was investigated in this work. The accuracy and probe path length of sphericity measurement were studied collectively to reduce measuring time. Three types of sampling strategies and six different sample sizes were addressed in conjunction with the determination of an optimal sample point sequence. A geometrical procedure for three dimensional arc length calculation was proposed to find distances between the sampled points along the curved surface. The concept of the traveling salesman problem (TSP) was then applied next. A relatively new discrete optimization algorithm, ant colony system (ACS), was easily adopted to find an optimal path sequence due to its appealing properties for solving TSP problems, such as near-optimal solutions, consistent results, and ability to handle large sample sizes. The obtained sequence was then employed by a CMM to actually measure the manufactured hemispherical surface. Influence of accuracy and path length was combined by using a priority coefficient to select an effective and efficient sampling strategy. Preliminary observations revealed that the Hammersley sampling method was very attractive in most test cases.

Keywords: Coordinate Metrology, Hammersley Sampling Strategy, Ant Colony System, Minimum Tolerance Zone, Traveling Salesman Problem

1. Introduction

Inspection is one of the most important processes in manufacturing. Probe-type coordinate measuring machines (CMMs) have been widely used for discrete part inspection due to their ability to handle a variety of features of manufactured products and their measurement accuracy. To improve effectiveness and efficiency of inspection by using CMMs, sampling methods and sample sizes that can obtain the maximum representative information from a population with least possible time, have been investigated in the literature. Several types of sampling strategies are employed such as simple random sampling, uniform sampling, and Hammersley sequence sampling. The appropriate sampling method is normally selected according to the accuracy requirement, the time requirement, the geometry features of the

workpiece, and the condition of the machine used to produce the workpiece. Sample size is typically proportional to time and hence cost. Savings in time may be achieved through a reduction of sample size with some mathematical sequence based sampling methods while still maintaining a high level of accuracy.

The development of formal procedures for effective and efficient sampling in dimensional measurement of three dimensional geometries such as conical and hemispherical objects was investigated by Lee et al. [1]. A mathematically sequence-based sampling method such as the Hammersley sampling strategy showed superior results to those of the most widely used sampling technique in practice, the uniform sampling method, in terms of accuracy and sample size. In other words, more information could be extracted by the Hammersley method when the same sample size was used [2-3]. Prakasvudhisarn and Raman [4] applied such a sampling method to experimentally collect data for form tolerance inspection of conical features as a well. Similarly, an inspection of a linearly approximated torusity model was also investigated by using various sampling methods [5]. In addition, Kunnapapdeelert and Prakasvudhisarn [6] investigated an optimal sample size selection for a true nonlinear torusity estimation by using neural networks. Most of these studies relied on computer simulation of pseudo-random surfaces and did not verify their results with measurement of actual surfaces. Therefore, CMM probe path planning was not really considered.

CMM tool path planning allows the determination of the inspection path joining the CMM measurement points based on the geometry of the inspected part model and the inspection specification. Few works have been done in the development of the CMM probe path planning. Lim and Menq [7] studied the accessibility of CMMs and its path generation in dimensional inspection. Probe orientation was considered for feature accessibility while attempting to decrease chances of collision. An improved path could then be generated accordingly. Lu et al. [8] developed an algorithm for generating an optimum collision-free CMM inspection path by using a modified three dimensional (3D) ray tracing technique. Yau and Menq [9] presented a hierarchical planning system for dimensional inspection using heuristics for CMMs path planning. The objective was to automate the planning of a collision-free inspection path for dies and molds. A simple path planning procedure was also proposed to automatically collect data and avoid obstacles for various sampling methods attempted in conicity measurement [4]. The majority of the studies has concentrated on generating the collision-free inspection paths for parts having multiple surfaces. They relied on both computer simulation and experimental tests to demonstrate effectiveness of their planned paths.

Generally, the probe controlled by an operator or a parts program moves from one point to the next without any particular order. Further efficiency can clearly be obtained by moving the probe to collect every point along a path having the shortest tour length. As mentioned earlier, the sample size and sample point locations play an important role for accuracy of form tolerance measurement. Therefore, to enhance inspection processes, both factors, accuracy of form tolerance measurement and total path length, should be investigated together. Coupled with flatness measurement accuracy, Kim and Raman [10] discussed the length of probe path with reference to sampling strategies and sample sizes on plates. The Euclidean distances between measured points on the same plane were directly analyzed for the shortest total tour length. Therefore, the CMM probe path problem was easily formulated as a

traveling salesman problem (TSP). However, for complex features like cones and spheres, the distance calculation of measured points and the obstacle avoidance movement of the probe together pose high degrees of difficulties and have been largely ignored in the coordinate form literature. A hemispherical surface is one of the most common features produced in many applications such as molds and bearings. Hence, the logical extension of sampling time reduction, which still considers accuracy and total probe path length, to form tolerance verification of hemispherical object is clearly desired.

This work has studied the issues of accuracy of sphericity measurement, as evaluated by minimum zone approach [11-13], and the length of probe path with reference to the sampling strategy and sample size. The calculation of the arc distance between two points in 3D space was proposed. The probe path movement along the curved surface possesses similar characteristics as the TSP problem. Subsequently, a good discrete optimization algorithm, the ant colony system (ACS), was selected to solve this TSP problem for an optimal path sequence of those sampled points due to its appealing advantages, such as near-optimal solutions, consistent results, and ability to handle large numbers of cities or sample sizes [14-17].

The sampling locations and sequence were then fed to a CMM for data collection. This was done by writing a parts program to control CMM directly and automatically. The data collected were then fit to verify the inspected geometry for form (sphericity) by using the minimum tolerance zone approach [18]. The minimax model was used as a criterion for best fit with the normal deviation model developed for this particular form. This was obtained by considering the difference between an actual measurement and a corresponding point on the ideal hemispherical surface [13]. The least square fit was not selected because of its occasional overestimation and normal distribution assumption [19].

In summary, the purpose of this work was to guide the selection of an effective and efficient sampling method for hemispherical feature inspection in the context of accuracy, number of inspected points, and total tour length of probe path. To do so, the following steps were investigated; (1) determination of proper sampling locations for such features; (2) development of an analytical model for three dimensional arc length calculation; (3) probe path optimization of the TSP based tool path problem; and (4) selection of a sampling strategy based on the combined effects of accuracy and total path length.

2. Sampling methods

To decrease inspection time while maintaining a high level of accuracy, various sampling techniques such as simple random sampling (SR), aligned systematic sampling (AS), and mathematically sequence-based Hammersley sampling (HM) have been studied. Interestingly, the root-mean-square errors of this mathematical sequence are lower than those of commonly practiced procedures, SR, and a type of AS, uniform sampling. Hence, HM, AS, and SR sampling methods were taken into consideration.

2.1 Hammersley based method

The HM sequence technique was designed to place N points on a k-dimensional hypercube [3]. In two dimensions, the HM coordinates (x_i, y_i) can be determined as follows:

$$x_i = \frac{i}{N} \quad (1),$$

$$y_i = \sum_{j=0}^{k-1} b_{ij} 2^{-j-1} \quad (2),$$

where N is the total number of sample points,

$$i \in I = [0,..., N-1],$$

k is $\lceil \log_2 N \rceil$ = ceiling of $\log_2 N$,
b_i is binary representation of the index i,
b_{ij} denote the j^{th} bit in b_i, and
j = 0,…, k-1.

2.2 Aligned systematic sampling method

The systematic sampling sequence is a form of probabilistic sampling which employs a grid of equally spaced locations. There are two types of systematic sampling; aligned and unaligned sampling. Aligned sampling is normally called systematic sampling. The sample is first determined by the choice of a pair of random numbers in order to select the coordinates of the upper left unit and the subsequent points are taken according to the predetermined mathematical pattern.

Suppose that a population is suggested in the form of *am* rows and each row consists of *bn* units. The basic procedure for arranging the coordinate of aligned systematic sampling can be computed as follows:

1. Determine a pair of random numbers (p,q) where p is less than or equal to m, and q is less than or equal to n. These random numbers would decide the coordinates of the upper left unit by the p^{th} unit column and q^{th} unit row.

2. Locate the subsequent sampling points for x-coordinate as $p+im$ where $i \in [0,...,a-1]$. Therefore, the row consists of $p, p+m, p+2m,..., p+(a-1)m$.

3. Locate the subsequent sampling points for y-coordinate as $q+jn$ where $j \in [0,...,b-1]$. Therefore, the column consists of $q, q+n, q+2n,..., q+(b-1)n$.

2.3 Simple random sampling method

Simple random sampling is the sampling procedure that each search element in the population has an equal chance of being selected.

The above sampling strategies are normally described for a 2 dimensional (2D) rectangle, but the hemispherical feature is a 3D problem. Extension from 2D space to 3D space is required. Since a hemisphere's profile contains a circular feature when considered from its top view, it is simpler to work with the 2D Polar coordinates (r_i, θ_i) than the 2D Cartesian coordinates (x_i, y_i). The rationale behind the following equations are that the area (A) of a circular surface is proportional to the square of its radius (R), $A = \pi R^2$ implies that $A \propto R^2$, and a circle can be easily divided into N sections equally [1]. Thus, the Polar coordinates of a Hammersley point on a circular surface are determined as follows:

$$r_i = y_i^{1/2} R \quad (3)$$

$$\theta_i = 360° x_i \quad (4)$$

where R is the radius of the circle. Equation (3) generates concentric circles whose radii are varied according to y_i's. Note that a specified measuring point is selected at the central point (0, 0) of a circular feature surface.

Similarly, the method of calculating the Polar coordinates of a Hammersley point on a hemispherical surface is very similar to that on a circular surface with an additional axis (Z axis). The area of a hemispherical surface is proportional to the square of its radius of base, $A = 2\pi R^2$, where R is the radius of the sphere. This implies that $A \propto R^2$. Therefore, the actual coordinates of the Hammerley points are just the projection of those points on the circular surface to the real hemispherical surface. Since a hemisphere is a 3D feature, the sampling points are defined as (radius, degree, height) or (r_i, θ_i, h_i), where $0 \le r_i \le R$, $0 \le \theta_i \le 360°$, and $-R \le h_i \le 0$. The origin (0, 0, 0) is set at the apex of a hemisphere. Thus, the Polar coordinates of a Hammersley point on a hemispherical surface are determined as follows:

$$r_i = (1-(1-y_i)^2)^{1/2} R \quad (5)$$

$$\theta_i = 360° x_i \quad (6)$$

$$h_i = -y_i R \quad (7)$$

Equations (3) to (7) were applied to locate sampling points for the other two sampling methods as well.

3. Arc distance calculation

Traditionally, an effective sampling method like HM can improve form tolerance inspection via CMMs as opposed to widely used sampling methods such as AS and SR [4, 5, 10]. The HM can maintain the same level of accuracy as other sampling strategies do with a fewer number of measured points. In other words, using the same sample size, the HM can extract more representative information from the inspected part than others can. However, the total path length of HM points may not be the shortest, especially when compared with that of the orderly uniform structure points based on the AS method [10]. Consequently, the inspection time that can be saved through a reduction of sample size may have to be spent more on traveling around the workpiece. Therefore, the shortest tour length of each sampling strategy needs to be determined so that an efficient path planning can be achieved. To do so, an arc distance between two measured points must be calculated first.

Generally, the CMM probe travels along a straight line for positioning before actually measuring the inspected workpiece. This movement gives the shortest distance between a starting point and an ending point, and it is not difficult technologically for a CMM manufacturer to implement this linear movement feature. Without the arc movement ability, some intermediate points are traditionally needed while inspecting circular-like object to prevent the probe from crashing with it. To reduce the number of intermediate points, a large clearance between probe and the workpiece is normally used. Obviously, this procedure is not efficient and also interferes with actual path length calculation between two measured points. Recently, arc movement has been implemented in modern CMMs. This provides an opportunity to efficiently plan CMM probe path for circular-like objects. Path planning, which is normally handled by using Euclidean distance calculation, does not fit well with hemispherical feature measurement. A 3D arc length calculation along a circular surface is clearly desired. Determination of this arc distance between a pair of points $i(x_i, y_i, z_i)$ and $j(x_j, y_j, z_j)$ is done by developing the following set of equations. Firstly, the sample points generated by a covered sampling method are converted to Cartesian system. Secondly, the Euclidean distance between these two points are calculated as follows:

$$Eu\_dist_{ij} = [(x_i - x_j)^2 + (y_i - y_j)^2 + (z_i - z_j)^2]^{\frac{1}{2}} \quad (8).$$

The obtained outcome is the shortest linear distance between these two points. Next, these two points and the center of a sphere at (0, 0, -*R*) form an isosceles triangle as shown in Figure 1. Let α be a vertex angle at the center of the sphere. It can be described as:

$$\alpha = 2\sin^{-1}\left(\frac{Eu\_dist_{ij}}{2R}\right) \quad (9).$$

Hence, the arc distance between points *i* and *j*, arc_dist_{ij}, can be determined as:

$$arc\_dist_{ij} = \frac{\alpha 2\pi R}{360^\circ} \quad (10).$$

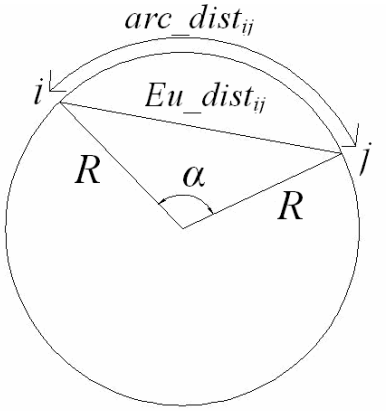

Figure 1. 2D view of arc length calculation of 3D hemisphere.

Thus, distances between every measured point on a hemispherical surface could be calculated. The obtained distances and their corresponding points can then be formulated as a TSP problem for CMM probe path planning. After solving the TSP problem, a sequence of points with the shortest tour length is applied to guide the probe for actual measurement. MATLAB® 7.0.4 was used to generate coordinates according to covered sampling methods with various sample sizes. In addition, it was also used to calculate a set of arc distances between generated coordinates. Note that a personal computer with Pentium IV 2.8GHz, 1GB RAM, and Microsoft Windows XP operation system was used to compute all equations and algorithms investigated in this work.

4. TSP algorithms

The shortest tour length is a result from an optimal sequence of collected points. This sequence taken by the probe is analogous to an optimal sequence of visited cities taken by a salesman. Thus, this probe path problem was approached as a TSP problem. The employed algorithms for tour construction were nearest neighbor heuristic (NN) and ant colony system (ACS).

4.1 Nearest neighbor (NN)

The nearest neighbor algorithm is one of the first and easiest algorithms used to find a solution to the TSP problem. This heuristic quickly yields an acceptable short tour due to its greedy nature. Its main idea is to select the nearest unvisited city as the next destination until the tour is complete. Steps are as follows:

1. Randomly select an initial city.
2. Search the nearest unvisited city. Ties are broken arbitrarily.
3. Move to the obtained city above.
4. If all cities have been visited, then terminate.
5. Otherwise, go to Step 2.

The sequence of the visited cities is a solution from the algorithm. Note that the NN heuristic is fallible since it does not always find the shortest path. Therefore, to further enhance the obtained solution, this algorithm should be combined with other algorithms.

4.2 Ant colony system (ACS)

The ACS is a meta-heuristic, behaviorally inspired by ants searching for food. A pheromone trail is normally used to communicate between them while finding the shortest path to the food source. As they travel, pheromone is laid down on the trail and evaporates over some period of time. If the shorter path is taken, the amount of evaporated pheromone is smaller. Other ants then can follow such a path. Thus, pheromone is gradually accumulated after multiple ants have been using the path. Eventually, the strongest pheromone path will emerge. This implies that the near-shortest or shortest path is found. This concept can be applied to solve combinatorial optimization problems such as TSP problems with very good outcomes [14-17]. Hence, the ACS was selected to improve the solution obtained by the NN algorithm. That is, the solution from the

NN algorithm was set as an initial pheromone path for the ACS algorithm. The steps of the ACS algorithm are well documented in the literature and not repeated here. The parameters of ACS used in the following experiments were $\alpha = 1$, $\beta = 2$, $\rho = 0.1$, $\xi = 0.1$, and $q_0 = 0.9$. In addition, the τ_0 was set to $(n*L_{nn})^{-1}$ where n was the sample size and L_{nn} was the tour length produced by using the NN algorithm. The number of ants (m) and the number of iterations were 10 and a minimum of $\{10000\frac{n}{m}, 100000\}$, respectively. These parameters were initially selected based on literature and eventually fine tuned for this particular application by using a trial and error approach. The implementations of both algorithms were done by using MATLAB® 7.0.4. The distances calculated previously were then fed to both algorithms for an optimal sequence of CMM probe path.

5. Selection of a sampling method

Three hemispherical specimens with diameter of 100 mm were used for data collection. They were made from S45C steel by using a CNC lathe Excel SL500. A 10 mm approach distance was used to prevent the probe from crashing with the inspected object while traveling. Therefore, the diameter of the simulated hemisphere was 120 mm. Five random orientations about the Z axis of CMM were applied to each specimen during data collection to avoid any systematic errors that may result from the manufacturing operation used. As mentioned earlier, the NN algorithm was initially applied to determine the length of the probe path. Its result was then incorporated, as an initial pheromone path, to the ACS algorithm. The obtained sampling sequence and sampling locations were then fed to CMM Mitutoyo Beyond A504 for data collection. A parts program was written to control the path movement of the probe so that the probe could move to the desired destination along the curved surface. The collected data points were next fit to verify the form of the inspected geometry, minimum tolerance zone sphericity.

The minimum zone approach recommended by [18] was used to verify the manufactured part. A tolerance zone of spherical feature is the smallest normal gap between a pair of concentric spheres covering all measurements. These imaginary spheres and an ideal sphere, which lies right in the middle between this pair, are established by using a minimax criterion [13]. The minimax criterion can be applied to other form features as well. The deviation model of each feature, however, is different. Since a hemisphere is a half of a sphere, the following deviation model of sphere was then used:

$$d_i = \sqrt{(x_i - x_o)^2 + (y_i - y_o)^2 + (z_i - z_o)^2} - R_o \quad (11)$$

where (x_o, y_o, z_o) represents the searched center of the hemisphere,

R_o denotes radius of hemisphere,

(x_i, y_i, z_i) is a measured point i, and

d_i is a normal distance between a measurement and a corresponding point on the ideal hemisphere.

This geometrical fitting was computed by using LINGO, an optimization package.

Table 1 depicts average results of five experiments with five orientations of these three specimens. Compared with the NN algorithm, the ACS algorithm found shorter average distances for all sampling methods attempted; except in a couple cases of 32 and 64 sample sizes for the AS method, and in a case of 8 sample size for the SR method. Generally, ACS could further improve the NN results, especially for the HM sampling strategy. Average distances of complete tours by the AS sampling strategy were generally shorter than those of the SR and HM methods due

to their exact distances between points. The HM method provided the longest tour paths in almost every case. The AS method was generally more efficient (shorter CMM probe path) than the other two sampling methods for hemispherical feature inspection.

To consider form measurement accuracy, average minimum zone solutions from each sampling method in Table 1 were comparatively analyzed. Note that the form inspection is a process of identifying errors or deviations unavoidably built into the manufactured workpiece. Hence, the larger the deviation found, implies the more effective the inspection method. Therefore, the accuracy of the HM method for sphericity inspection was much superior to that of the AS and SR methods in every sample size, especially when low and medium sample sizes were used. The SR sampling method also performed better than the AS method in terms of measurement accuracy. The computed tolerance zone relied mainly on extracted information (or locations of measured points) from the inspected object. This implies that the HM strategy could provide more information of the workpiece than the others. If the same level of inspection accuracy is desired, the HM method can be used to generate measured points with smaller sample size. This should also result in shorter traveling time of the probe and faster inspection time due to less number of points measured.

The trade-off between these sampling methods in terms of accuracy and probe traveling time was apparent. This could be further investigated by using a trade-off quantification proposed by [10]:

$$S = (100 - Ra) * b + (100 - Rp) * (1 - b) \quad (15)$$

where S is the sampling methods selection measure or sampling efficiency,

Ra is the discrepancy rate of accuracy of sphericity,

Rp is the relative length rate of the length of CMM probe path,

b is a [0, 1] priority coefficient which indicates the priority of accuracy versus length;

$$Ra = \frac{(a - c)}{a} 100 \quad (16)$$

where a is the highest achievable average accuracy of all specimens among all sample sizes and sampling methods,

c is an actual average accuracy obtained through the experiment; and

$$Rp = \frac{n}{m} 100 \quad (17)$$

where n is an average distance of the actual path obtained through the experiment,

m is the longest average path among all sample sizes and sampling strategies.

The discrepancy rates (Ra) of all sampling strategies for every sample size are illustrated in Table 2. The relative length rates (Rp) are depicted in Table 3. Figures 2 and 3 show a graphical comparison between discrepancy rates and sample sizes for every sampling method and a graph of relative length rates versus samples sizes of all sampling methods, respectively. Based on Equations (16) and (17), small discrepancy rate (Ra) and small relative length rate (Rp) are preferred because these imply high average accuracy and short average traveling distance, when relatively compared with the best values obtained from all specimens and all sample sizes and sampling strategies.

Clearly, the most suitable sampling strategy is the one that minimizes inspection time and maximizes measurement accuracy simultaneously. Consideration of only sample size, regardless of sampling sequence for measurement time, can mislead the selection of such a sampling method. To combine these factors, the priority coefficient is based on the policy of the quality control (QC) department during planning. To determine a proper sampling method in the light of accuracy and measuring time, the priority coefficient was varied from 0 to 1 and tabulated in Table 4 with a step size of 0.2.

Table 1. Average distances and minimum zone results in millimeter of five experiments with five orientations of the specimen using AS, HM, and SR sampling strategies.

Sam-ple sizes	Avg. distances using AS		Avg. distances using HM		Avg. distances using SR		Avg. min. zones using AS	Avg. min. zones using HM	Avg. min. zones using SR
	NN	ACS	NN	ACS	NN	ACS			
8	463.901	447.557	481.652	441.804	379.158	379.158	0.0063	0.2706	0.0807
16	533.641	498.877	670.748	601.025	486.494	473.357	0.0926	0.3137	0.1335
32	761.631	761.631	941.627	842.822	713.887	681.332	0.1049	0.3298	0.2220
64	795.494	795.494	1348.838	1167.153	1075.575	967.514	0.1595	0.3379	0.2652
128	1264.292	1252.026	1834.835	1625.900	1552.520	1274.890	0.2744	0.3428	0.2888
256	1438.655	1428.573	2527.877	2290.090	2030.666	1784.097	0.2868	0.3471	0.3053

Table 2. Average discrepancy rates of accuracy of sphericity by sample sizes and sampling strategies.

Sample size	Sampling strategy		
	AS	HM	SR
8	98.1338	20.9065	78.0526
16	74.4649	9.6712	62.3947
32	70.8203	4.9742	36.7367
64	55.1007	2.7330	24.2963
128	21.3972	1.1855	17.6285
256	18.6119	0.0000	12.8008

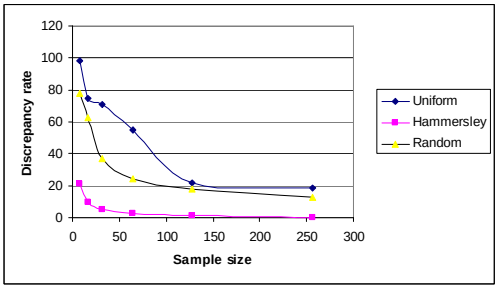

Figure 2. Comparison of average discrepancy rates by sample sizes and sampling strategies.

Table 3. Relative length rates of CMM probe path length by sample sizes and sampling strategies.

Sample size	Sampling strategy		
	AS	HM	SR
8	19.5432	19.2920	16.5565
16	21.7842	26.2446	20.6698
32	33.2577	36.8030	29.7513
64	34.7364	50.9654	42.2478
128	54.6715	70.9972	55.6699
256	62.3807	100.0000	77.9051

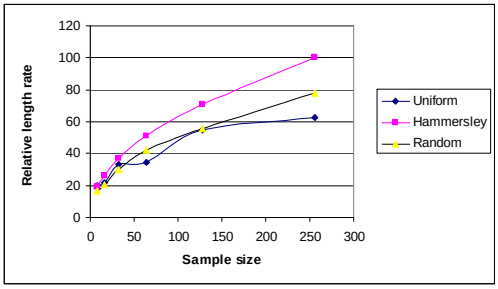

Figure 3. Comparison of average relative length rates by sample sizes and sampling strategies.

Table 4. Sampling methods selection measured by the trade-off between the accuracy of sphericity and the length of CMM probe path.

Sample size	*b*	Sampling strategy		
		AS	HM	SR
8	0.0	80.4568	80.7080	83.4435
	0.2	64.7387	80.3851	71.1443
	0.4	49.0206	80.0622	58.8451
	0.6	33.3025	79.7393	46.5459
	0.8	17.5843	79.4164	34.2467
	1.0	1.8662	79.0935	21.9474
16	0.0	78.2158	73.7554	79.3302
	0.2	67.6797	77.0701	70.9852
	0.4	57.1435	80.3848	62.6402
	0.6	46.6074	83.6994	54.2953
	0.8	36.0712	87.0141	45.9503
	1.0	25.5351	90.3288	37.6053
32	0.0	66.7423	63.1970	70.2487
	0.2	59.2298	69.5628	68.8516
	0.4	51.7173	75.9285	67.4545
	0.6	44.2047	82.2943	66.0575
	0.8	36.6922	88.6600	64.6604
	1.0	29.1797	95.0258	63.2633
64	0.0	65.2636	49.0346	57.7522
	0.2	61.1908	58.6811	61.3425
	0.4	57.1179	68.3276	64.9328
	0.6	53.0450	77.9741	68.5231
	0.8	48.9721	87.6205	72.1134
	1.0	44.8993	97.2670	75.7037
128	0.0	45.3285	29.0028	44.3301
	0.2	51.9834	42.9651	51.9384
	0.4	58.6382	56.9275	59.5467
	0.6	65.2931	70.8898	67.1550
	0.8	71.9479	84.8522	74.7632
	1.0	78.6028	98.8145	82.3715
256	0.0	37.6193	0.0000	22.0949
	0.2	46.3731	20.0000	35.1158
	0.4	55.1268	40.000	48.1366
	0.6	63.8806	60.0000	61.1575
	0.8	72.6343	80.0000	74.1783
	1.0	81.3881	100.0000	87.1992

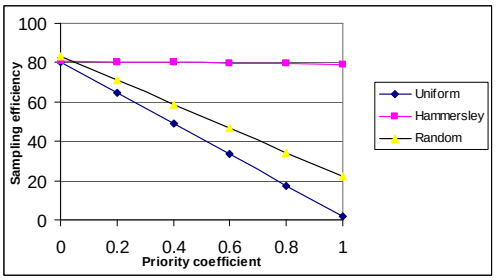

Figure 4. Comparison of sampling efficiency by priority coefficients and sampling strategies at sample size of 8.

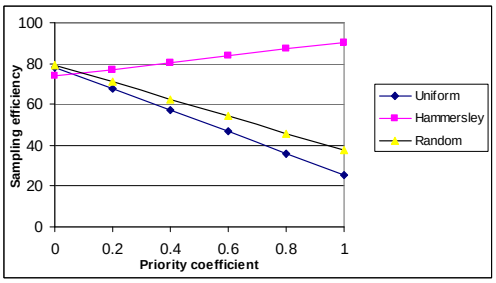

Figure 5. Comparison of sampling efficiency by priority coefficients and sampling strategies at sample size of 16.

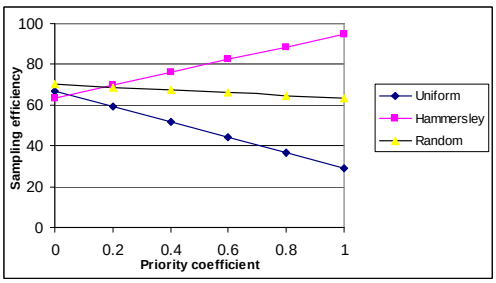

Figure 6. Comparison of sampling efficiency by priority coefficients and sampling strategies at sample size of 32.

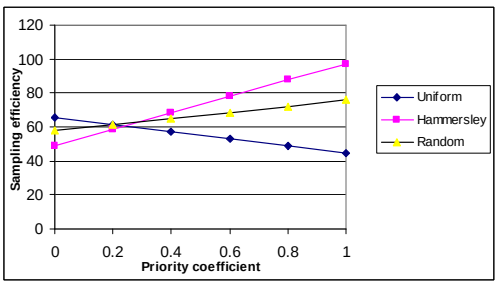

Figure 7. Comparison of sampling efficiency by priority coefficients and sampling strategies at sample size of 64.

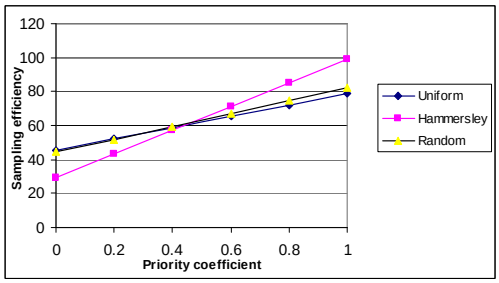

Figure 8. Comparison of sampling efficiency by priority coefficients and sampling strategies at sample size of 128.

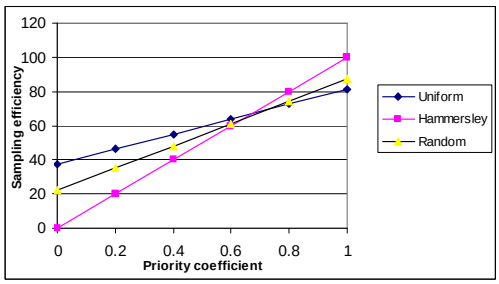

Figure 9. Comparison of sampling efficiency by priority coefficients and sampling strategies at sample size of 256.

Sampling efficiencies of the studied sampling methods with various priority coefficients are depicted in Figures 4-9. The low priority coefficient (0 or 0.2) represents the emphasis by the QC department on short traveling distance or low traveling time of the CMM probe. The medium priority coefficient (0.4 or 0.6) focuses on the balance between the accuracy of hemispherical measurement and the total CMM probe path length. Lastly, the high priority coefficient (0.8 or 1.0) implies the highlight on the accuracy of form measurement with little or no regard for the probe path length. Figure 4 illustrates that the HM method gave the highest results at almost every value of *b*'s. Only the SR method at $b = 0$ could slightly outperform the HM method. The SR (random) and the AS (uniform) methods declined drastically with a higher range of *b*'s. In addition, the SR method exhibited better results than the AS method. These observations showed that the HM method was very attractive for a very small sample size of 8 when probe traveling distance and measurement accuracy were both taken into consideration. The main reason was the dominance of accuracy of the HM method over the accuracy of the other two methods while probe traveling times of each method were not much different, due to the small sample size employed. Therefore, different values of *b* did not produce much different results for sampling efficiency of the HM method. On the contrary, low priority coefficient reflected high sampling efficiency for the SR and AS methods since their strengths lay on the short path length, not on accuracy. Hence, when accuracy was the main concern (high priority coefficient), they gave low sampling efficiency. Figures 5-9 also show similar patterns. Hence, similar analyses to those of Figure 4 can also be made. In Figure 5, the HM method obviously outperformed the other two methods but the gaps between them were narrower than those in Figure 4. Every sampling method generally produced better results than those in Figure 4, except for $b = 0$. Similar patterns also appear in Figures 6-9. At the lower end of *b*'s, sampling efficiencies decreased and vice versa. Sampling efficiencies of the HM method decreased at a faster rate for low *b*'s than those of the other two methods for larger sample sizes. They also increased at a faster rate for high *b*'s than those of the other two methods. In other words, for the emphasis on short distance (low *b*'s), the HM method, which gave the longest traveling distance for medium to large sample sizes, would give the lowest sampling efficiencies. On the other hand, for the highlight on accuracy (high *b*'s), the HM method, which presented the most accurate results, would give the highest sampling efficiencies.

These can be clearly seen in Figures 6-9, especially in Figure 9.

Intuitively, the increase of sample size will increase the probe traveling distance and also improve the measurement accuracy of each method. These can be observed clearly across Figures 4-9. At low priority coefficient, the sampling efficiencies decreased because probe path length increased due to the use of higher sample sizes. Moreover, at higher priority coefficient, the sampling efficiencies increased because measurement accuracy improved over the larger sample sizes.

It was also observed across Figures 4-9 that a smaller sample size and lower *b*'s showed a higher sampling efficiency for every sampling method because a smaller sample size would generally produce lower traveling distance and lower *b*'s emphasized length, not accuracy. Moreover, a larger sample size and higher *b*'s depicted a higher sampling efficiency for every sampling strategy, because a larger sample size would generally produce higher measurement accuracy, and higher *b*'s focused more on accuracy, not on distance. The HM strategy was very attractive, especially for a low sample size and became less dominant for a very high sample size. In addition, the variations of sampling efficiencies of these methods were relatively high for a small sample size and were much narrower for a large sample size. This implies that for a large sample size the role of sampling strategies or point locations in hemispherical measurement is decreased and the significance of this large sample size has gained dominance in measurement. Based on the results and analyses above, a summary of sampling methods selection from Table 4 and Figures 4-9 can be tabulated in Table 5. From Table 5, when high measurement accuracy was concerned, the HM method should be chosen. The HM method remained attractive, but became less dominant for a larger sample size. The consideration of both traveling distance and measurement accuracy showed that the HM method was still a method of choice, especially for low to medium sample sizes. The AS and SR methods could also be selected for medium to high sample sizes without much difference. The emphasis on traveling distance made the AS method attractive for every sample size. In addition, it was the obvious option for a very large sample size. The SR method could be chosen for low to medium sample sizes. Moreover, the HM method was suitable for only low sample sizes since it produced the greatest traveling distance among all three sampling strategies.

Table 5. Summary of sample sizes and sampling methods selection for hemispherical feature inspection.

Sample size	Inspection emphasis		
	Low traveling time	Medium traveling time and accuracy	High measurement accuracy
8	HM, AS, SR	HM	HM
16	HM, AS, SR	HM	HM
32	HM, AS, SR	HM	HM
64	AS, SR	HM, SR	HM
128	AS, SR	HM, AS, SR	HM
256	AS	HM, AS, SR	HM, AS, SR

6. Discussion

Measurement accuracy and time are important factors for form inspection using CMMs. Therefore, sampling strategies and their sample sizes have been investigated for some specific form features in the literature [4, 5, 10]. The CMM probe path has been largely ignored despite its major influence on inspection time due to the geometrical complexity of

inspected features. The simple arc distance calculation proposed in this work could bridge the gap and make the investigation of sphericity inspection thorough. An effective and efficient inspection plan should provide a major impact for industry since a hemispherical feature is very common in many applications. The reference frame of CMMs can be set up at the early stage of inspection for this particular feature and this can establish the position of the inspected workpiece, its origin, and coordinates generated by the sampling methods.

As mentioned earlier, the ACS algorithm was adopted due to its appealing properties such as near-optimal solutions, consistent results, and ability to handle large sample sizes. Its computational time does not play a key role here because the inspection planning, including the specified sampling method and sample size, is normally done before the actual operation. Once the plan is complete, operators just follow the guidelines on the plan. Hence, the actual inspection time does not really include TSP algorithm's computational time.

Consequently, the selection of a proper sampling method could be studied and applied in practice. As clearly demonstrated for the first time in the literature, sampling methods, sample sizes, and sampling sequences contributed to the accuracy and speed of hemispherical feature inspection. These results strengthen the need for consideration of multiple factors in CMM sampling. Different methods are suitable at different sample sizes and different inspection preferences. The sample sizes studied were arbitrarily selected to represent typical sizes used in industry from small to large sizes and to provide some consistent basis for comparing alternate sampling sequences. As the sample size increased, the discrepancy rates of sphericity decreased and the length rates of probe path increased for all three sampling strategies. The HM method can be selected for most cases, especially when high measurement accuracy is concerned. The AS method can be chosen when the short probe path length is the priority due to the systematic nature of its generated points.

7. Conclusions

A data collection problem consisting of sample sizes, sample point locations, and sampling sequences was shown to collectively impact the inspection process. To balance the measurement accuracy and speed, a proper sampling method must be selected by considering these three factors together. A 3D arc length calculation was proposed to find distances between the sampled points for a hemispherical feature. An optimal path sequence could then be determined when the point locations and their distances were formulated as a TSP problem. A priority coefficient was used to combine influences of accuracy and path length of the covered sampling methods and sample sizes. Preliminary observations revealed that the Hammersley sampling method was very attractive in most test cases. The aligned systematic sampling method produced the shortest total distance of probe path. The procedure studied in this work is very useful for industry due to the abundant applications of hemispherical features.

These proposed guidelines can be expanded in the future to cover other form features such as cylinders, cones, and toruses. Their arc length calculations are clearly desired to compute distances between sample point locations. The sampling methods selection can be further enhanced by a better model representing inspection preferences.

8. Acknowledgments

The authors were partially supported by the Thailand Research Fund (TRF) grant MRG4980170 and Thammasat Research Fund 2550.

9. References

[1] Lee, G., Mou, J., and Shen, Y., Sampling Strategy Design for Dimensional Measurement of Geometric Features Using Coordinate Measuring Machine, Int. J. Mach. Tools and Man., Vol.37, No.7, pp. 917-934, 1997.

[2] Woo, T.C., and Liang, R., Dimensional Measurement of Surfaces and Their Sampling, Computer-Aided Design, Vol.25, No.4, pp 233-239, 1993.

[3] Woo, T.C., Liang, R., Hsieh, C.C., and Lee, N.K., Efficient Sampling for Surface Measurements, J. Man. Sys., Vol.14, No.5, pp. 345-354, 1995.

[4] Prakasvudhisarn, C., and Raman, S., Framework for Cone Feature Measurement Using Coordinate Measuring Machines, ASME J. Man. Sci. and Eng., Vol.126, No.1, pp. 169-177, 2004.

[5] Aguirre-Cruz, J.A., and Raman, S., Torus Form Inspection Using Coordinate Sampling, ASME J. Man. Sci. Eng., Vol.127, pp. 84-95, 2005.

[6] Kunnapapdeelert, S., and Prakasvudhisarn, C., Optimal Sample Size Selection, for Torusity Estimation Using a PSO Based Neural Network, Thammasat Int. J. Sci. Tech., Vol.12, pp. 64-77, 2007.

[7] Lim, C.P., and Menq, C.H., CMM Feature Accessibility and Path Generation. Int. J. Prod. Res., Vol.32, No.3, pp. 597-618, 1994.

[8] Lu, E., Ni, J., and Wu, S.M., An Algorithm for the Generation of an Optimum CMM Inspection Path. J. Dyn. Sys. Meas. and Con., Vol.116, No.3, pp. 396-404, 1994.

[9] Yau, H.T., and Menq, C.H., Automated CMM Path Planning for Dimensional Inspection of Dies and Molds Having Complex Surfaces. Int. J. Mach. Tools and Man., Vol.35, No.6, pp. 861-876, 1995.

[10] Kim, W.S., and Raman, S., On the Selection of flatness Measurement Points in Coordinate Measuring Machine Inspection, Int. J. Mach. Tools and Man., Vol.40, pp. 427-443, 2000.

[11] Kanada, T., Evaluation of Spherical form Errors-computation of Sphericity by Means of Minimum Zone Method and Some Examinations with Using Simulated Data, Prec. Eng., Vol.17, pp. 281-289, 1995.

[12] Fan, K.C., and Lee, J.C., Analysis of Minimum Zone Sphericity Error Using Minimum Potential Energy Theory, Prec. Eng., Vol. 23, pp. 65-72, 1999.

[13] Prakasvudhisarn, C., A Particle Swarm Search for Determination of Minimum Zone, Proc. 7th Int. Conf. Ind. Manage (ICIM), Japan, pp. 109-115, 2004.

[14] Dorigo, M., Maniezzo, V., and Colorni, A., Ant System: Optimization by a Colony of Cooperating Agents, IEEE Trans. Sys. Mans. Cyb., Vol.26, No.1, pp. 29-41, 1996.

[15] Gambardella, L.M., and Dorigo, M., Solving Symmetric and Asymmetric TSPs by Ant Colonies, IEEE Conf. Evol. Comp., pp. 622-627, 1996.

[16] Dorigo, M., and Gambardella, L.M., Ant Colonies for the Traveling Salesman Problems, BioSys., Vol. 43, No.2, pp. 73-81, 1997.

[17] Dorigo, M., and Gambardella, L.M., Ant Colony System: a Cooperative Learning Approach to the Traveling Salesman Problem, IEEE Trans. Evol. Comp., Vol.1, No.1, pp. 53-66, 1997.

[18] ASME Y14.5M-1994, Dimensioning and Tolerancing, The American Society of Mechanical Engineers, New York, 1995.

[19] Prakasvudhisarn, C., Trafalis, T.B., and Raman, S., Support Vector Regression for Determination of Minimum Zone, ASME J. Man. Sci. Eng., Vol.125, No.4, pp. 736-739, 2003.